29º Congresso Internacional de Transporte Aquaviário, Construção Naval e Offshore

Híbrido, 25 a 27 de outubro de 2022

Analysis and thermal characterization of Stud Welding in shipbuilding applications

Alisson Fernandes da Rosa – UFSC/LABSOLDA, Florianópolis/Brazil, alisson.fernandes@posgrad.ufsc.br
Régis Henrique Gonçalves Silva – UFSC/LABSOLDA, Florianópolis/Brazil, regis.silva@ufsc.br
Tiago de Siqueira Lima Marchione – UFSC/LABSOLDA, Florianópolis/Brazil, tiago.marchione@posgrad.ufsc.br
Ricardo Reppold Marinho - CENPES/PDIDP/TIA/TMI, Rio de Janeiro/Brazil reppold@petrobras.com.br
Giovani Dalpiaz - CENPES/PDIDP/TIA/TMI**,** Porto Alegre/Brazil, giovani.dalpiaz@petrobras.com.br

Abstract

The Stud Welding process is one of the welding technologies that are applied in shipbuilding and offshore. In this context, the objective of this study is to preliminarily evaluate the thermal behavior of the SW process for fastening threaded studs used in the off-shore sector in metallic structures where there is a restriction of thermal contribution on the back of the parts. The analyses were performed using thermocouples and the infrared thermography technique to measure the maximum temperature on the back of different plate thicknesses for different stud diameters. The study verified the maximum temperature reached and the evolution of the thermal behavior on the backside of the parts welded with SW. The results of this preliminary study show that depending on the thickness of the part to be welded, even with the reduced exposure time to the higher heat of the stud welding process, heating on the back of the part can be an imminent risk to the coating material, such as paint for example.

1. Introduction

The Stud Welding (SW) process was developed shortly before World War II and used by the U.S. Navy on military ships. The application was based on the proper fastening and installation of wooden decks that were still installed by thru-bolts on submarines, battleships, and aircraft carriers (Stanley 2022). Without SW this service required many hours of labor, including activities such as making and installing scaffolding to accommodate the nuts on the threaded bolts. In addition, the nuts were often welded to keep them from coming loose due to vibration. Today SW technology is widely used in various industry applications, such as welding components in the shipbuilding and construction sectors (Chambers, 2001), as well as the automotive sector (Ramasamy, 2002). Hsu and Mumaw (2011) presented a study that also employs stud welding for various advanced high strength steels (AHSS).

In the context of off-shore sector applications, demands such as heat input restriction and productivity improvement in the pinning of mechanical elements by welding have been identified, which can be satisfied with the SW process. An example of this is the modular metallic structures on oil platforms that have some insulating system or paint, or even welds on the walls of various hydrocarbon tanks that have a highly volatile and flammable characteristic.

It is important to emphasize that during the welding process of the studs, which can normally be from 3 to 25 mm in diameter and welded by fusion to the base metal, high welding currents are used, between 200 and 2500A in up to one second of welding time depending on the diameter (Nishikawa, 2003). In this sense, from the practical point of view of the process, even without the need to access the back of the plate to fix components such as threaded studs, the heat generated by the electric arc during welding can be a limiting factor, even during the manufacturing stage as well as in maintenance and repair operations, either because of the risk of degradation or the risk of explosion of the internal medium. Previous research has been conducted, however, only for 12,7 mm thick low carbon steel plates. Rosa et al. (2022) measured a temperature of approximately 105°C welding M10 studs and 206°C for M20 studs. In this context, from a practical point of view, the thermal behavior of the process was then first explored and investigated.

2. Metodology

To obtain temperature information prior to actual application, testing was conducted using 10 and 20 mm diameter threaded studs (M10 and M20, respectively) that were welded to 9,5, 12,7 and 15,9 mm thick low carbon (with 0,18%) ASTM A36 steel plate in the vertical welding position. Additionally, testing was also conducted using 16 mm diameter (M16) threaded studs in 7,9 mm thick low carbon (with 0,18%) ASTM A36 steel plate. The main objective of the temperature measurements on the backside of the SW welded steel plates was to obtain the maximum and cooling temperature curves by means of infrared thermography and thermocouples. The thermocouple measurements were performed before the plate was back-painted with a solvent-free, bi-component, intermediate, and high-thickness epoxy-polyamine primer formulated with non-toxic anticorrosive pigments for carbon steel surfaces. After painting, the thermal cycle was recorded using a thermographic camera. The welding source employed in all tests was a SOYER/BMK-16i equipped with a SOYER/PH-3N stud welding gun. A Flir/T1030sc thermographic camera was used to obtain the maximum and cooling temperature curves. K-type thermocouples were used, for verification and calibration purposes of the emissivity (ε) value. To validate the measurements taken, all tests were repeated to check the results. The main welding parameters used that are significant to this study are described in Table 1.

Table 1. – Welding parameters used

Parâmetros	M10	M16	M20
Welding Current (A)	790	800	970
Arc Time (ms)	350	500	920
Protrusion (mm)	2,5	2,5	1,5
Lift (mm)	1,5	2,0	5,0

3. Results

The temperature data was plotted in the form of a graph as a function of time for all studs and with the different plate thicknesses. It is possible to verify in Figure 1 the maximum temperature and the evolution of the thermal behavior of the welding in all tested conditions.

In general, the combinations of larger diameter studs with thinner plates showed higher temperatures, as expected, since larger diameter studs require higher levels of current and arc time in order to have an acceptable weld, as well as lower plates that have less material to dissipate the heat generated by the weld.

Therefore, the highest temperature measured on the back of the plate was for the M20 stud welded to 9,5 mm thick plate, where the maximum temperature reached approximately 402°C.

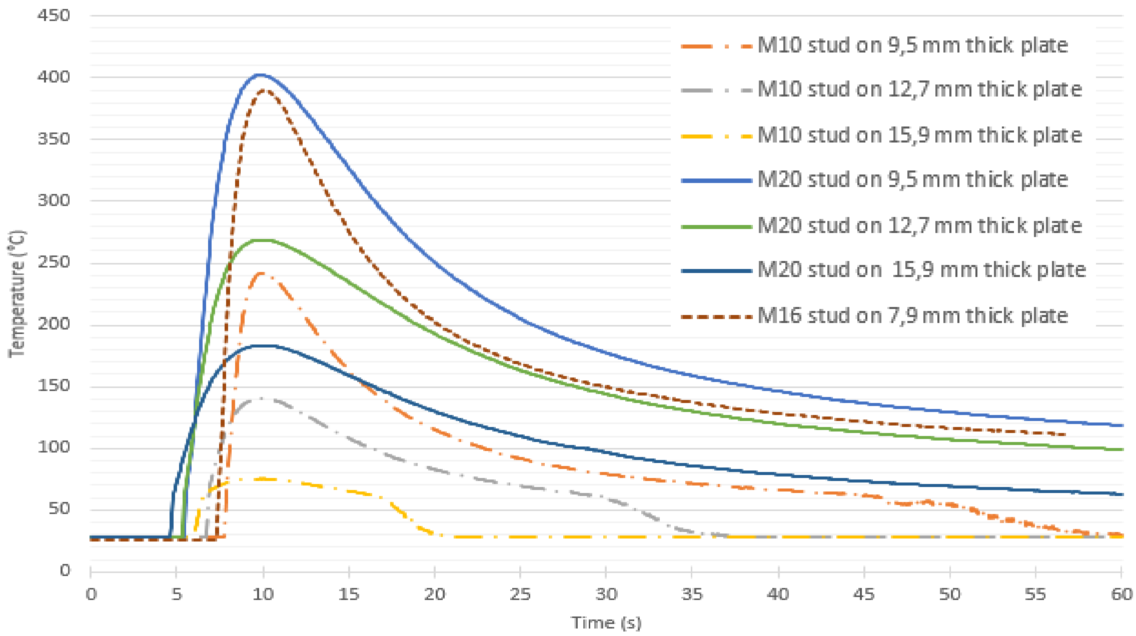

Figure 1 - Thermal cycle for all tested conditions.

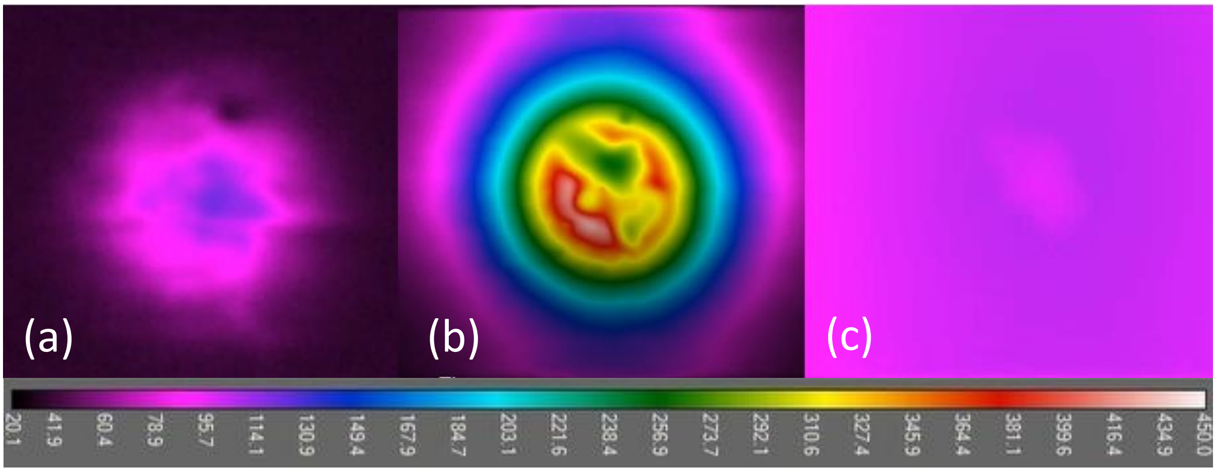

Figure 2 - Infrared thermography images at 3 different times: (a) at the moment of arc opening; (b) 500 ms after arc opening (maximum temperature); and (c) 60 s after arc opening.

After collecting the temperature curves for the different conditions tested, the back of the 7,9 mm thick plate was painted, in order to simulate a real situation in the application of stud welding in the offshore sector. It is important to emphasize that the specifications of the paint manufacturer and the N2628 technical standard were respected, especially regarding its application, the curing time between coats, and the total curing time. With the back of the painted plate, the welding of the M16 stud was performed again and monitored by infrared thermography.

Figure 2 illustrates the results of the infrared thermography filming performed on the painted plate. The evolution of the thermal behavior of the weld of the M16 stud on a 7,9 mm plate is evidenced in three different instants, recorded during and after welding the stud on the back of the plate, to enrich the visual analysis of the thermal behavior of the process.

Figure 2a illustrates the instant captured by the camera immediately after opening the arc in the Stud Welding process. At this instant, the camera registers a temperature of approximately 130°C in the center of the weld region.

Figure 2b illustrates the exact moment where the piece reaches the maximum temperature during the procedure, being registered in the infrared camera the temperature of 384.4°C. At this moment it is also possible to see the heat distribution along the part, represented by the isothermal lines, which show the temperature gradient at different levels and connect regions of the same temperature along a surface. During the execution of the procedure, the central region of the weld presents the highest temperature isotherm and decreases slightly from the center to the ends. Figure 2c illustrates the time after about 145 seconds of opening the arc, it is possible to observe that the plate is already with well distributed and uniform heat, with no temperature gradient, being recorded by the infrared camera a temperature of approximately 100°C. It is possible to observe in the center of the weld a region that represents the paint detachment in the form of bubble, caused by the heat generated by the welding arc.

To complement the understanding of the thermal cycle in this procedure, Figure 3 allows following the evolution of the temperature on the back of the plate, at the center point of the weld, which relates the temperature by the time during approximately 150 seconds. In this graph, the same points (a), (b) and (c) of the filming done with infrared thermography (presented in Figure 2) were marked.

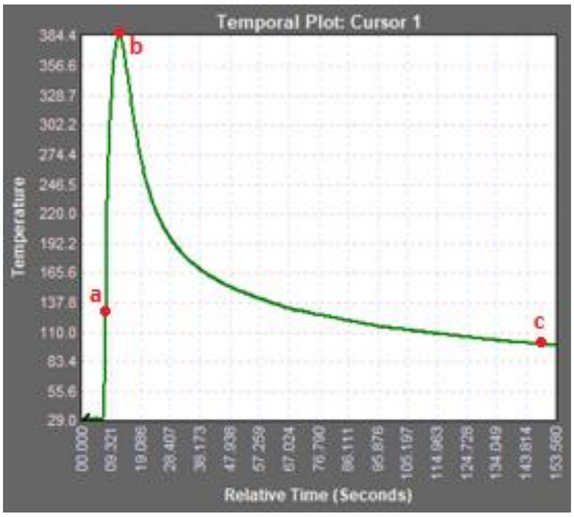

Figure 3 - Thermal cycling on the backside of the 7,9 mm thick plate at the center of the M16 stud weld

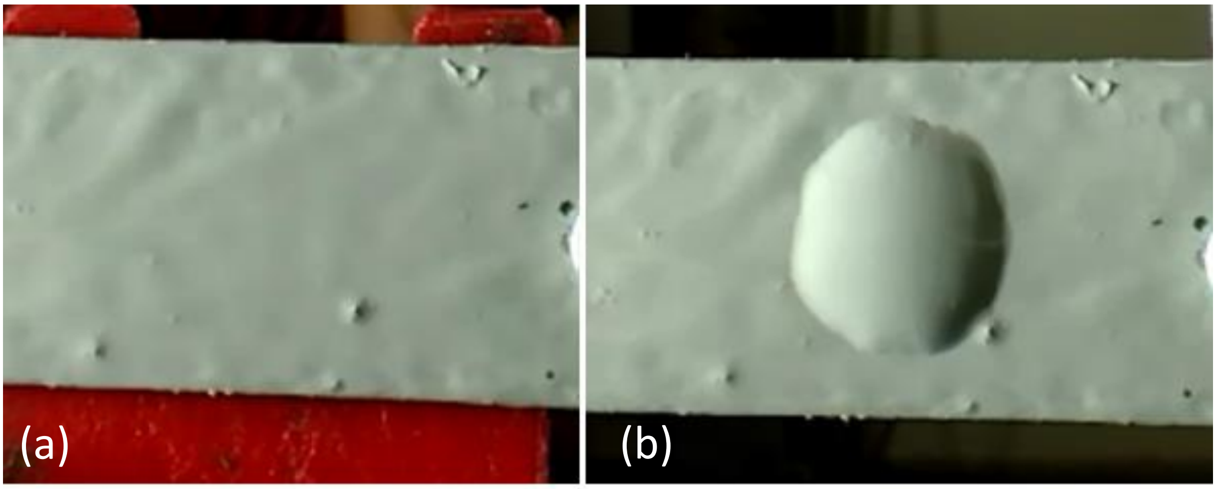

Figure 4 - Effects of arc-generated heat on the coating paint on the backside of the 7,9 mm plate welded with a M16 stud. (a) before welding, (b) after welding

Figure 4 illustrates the moment before and after welding the M16 stud. It is possible to observe the result of the heat generated by the arc of welding the M16 stud on the coating paint employed on the back of the 7,9 mm plate, where the maximum temperature recorded was approximately 385 C. This temperature degraded the paint applied, causing blistering and peeling of the paint, even though the heat was applied in a very short time (Arc time of 500 ms, as shown in Table 1).

4. Conclusions

Although this brief study presents only initial results about the heat generated and the consequences on the workpiece, it was possible to map a small application range of the SW process. This data will serve to assist in the combination and selection of stud diameters and plate thicknesses to be welded by the SW process, containing temperature operating ranges in various combinations. The data will serve as an additional tool for the operator to draw upon when selecting welding parameters and consumables.

In the footage taken with infrared thermography, it is evident that the region heated by the arc shot is concentrated in a region near the center of the welded stud and dissipates rapidly. Even though the procedure time is short compared to other conventional arc welding processes, in general, the temperatures obtained for larger studs in thinner sheets evidenced the degradation of the applied paint and seem to present potential risks to the materials positioned on the backside of the piece. Still, it is considered that further studies are essential regarding the operational limits between the heat generated and the degradation of the material applied to the back of metal structures, whether this material is a paint coating, or thermal/acoustic insulation, or a hydrocarbon with highly volatile and flammable characteristics.

5. References

STANLEY Engineered Fastening: Drawn Arc Stud Welding 08 Mai. 2022 https://www.stanleyengineeredfastening.com/resources/stud-welding-methods

CHAMBERS, H.A., 2001. Principles and Practices of Stud Welding. Pci Journal. Elyria, Ohio.

RAMASAMY, S. 2002. Drawn arc aluminum stud welding for automotive applications. JOM 54, 44–46 https://doi.org/10.1007/BF02711866

HSU, C.; MUMAW, J. 2011. Weldability of advanced high-strength steel drawn arc stud welding. Welding Journal, v. 90, p. 45-53,

NISHIKAWA, N. 2003. The principle and application field of stud welding, Welding international, 17:9, 699-705, https://doi.org/10.1533/wint.2003.3170

ROSA, A. F., BATISTA, F., BRASIL, L. M., ZANINI, J. B., SILVA, R. H. G. 2022 Preliminary Characterization of the Thermal and Electrical Behavior of Stud Welding. In: Proceedings ABCM - CREEM 2022, RS/Brazil